A Natural First Approximation to Low-Thrust Trajectories Between Satellite Orbits of the Earth and Moon

JOSEPH C. KING*

George C. Marshall Space Flight Center, Huntsville, Ala.

This paper describes a new technique for generating approximate low-thrust trajectories between satellite orbits of the earth and moon, using a series of two-body trajectories in combination with a systematic synthesizing process. The composite trajectories obtained by this method consist of constant tangential thrust powered spirals, one ascending and one descending for each one-way trip, joined by a connected pair of coasting arcs. The transition between the earth-influenced and moon-influenced portions of the physical model occurs at the junction of the two coasting arcs. The two-body powered trajectory segments are integrated numerically by a computer program, which also calculates regularly certain properties of the osculating Keplerian orbit corresponding to the instantaneous state of the vehicle. Families of these osculating orbits are later compared, obtaining matching conditions at the apoapsides of a particular pair of geocentric and selenocentric orbits. Since only apsidal points are matched, all coasting arc junctions fall along the earth-moon line (cislunar and translunar matches are possible). The paper presents the results of applying the synthesizing technique to the earth-moon transfer problem for a set of parametric variations in the powered spirals. The results are compared to previously published data, and an over-all evaluation is presented.

Nomenclature

c = propellant exhaust speed
ϵ = eccentricity
F = thrust
= thrust acceleration (F/m)
h = angular momentum
K = gravitational parameter
m = mass of vehicle
M = mean anomaly
n = mean motion
p = parameter (semilatus rectum)
r = radial distance
r_A = radial distance of apoapsis
R_M = earth-moon distance
t = time
T_{RC} = receding coast time (cutoff to apoapsis)
θ = angular displacement (powered trajectory)
v_A = speed at apoapsis
V_M = orbital speed of moon
Δv = velocity increment ($\int f\,dt$)

Introduction

THE potentialities of advanced, low-thrust propulsion systems in providing the logistic support for future lunar operations have been recognized for several years. A number of investigators have studied this application and reported their findings, and several (including London,[1] Stuhlinger,[2] Brown,[3] Battin,[4] and Donham[5]) have devoted considerable effort to the delineation of approximate trajectories. The trajectory studies have taken several rather different forms, and this aspect has made the present body of literature somewhat difficult to compare and interpret. A major problem is presented by the lack of a clear standard for comparison. Although much solid progress has been made over the last few years in the general field of low-thrust trajectory optimization (e.g., Irving[6] and Melbourne[7]), the methods used are not immediately applicable to the earth-moon situation.

The present study was undertaken as an effort to analyze the basic considerations involved in low-thrust flight between the earth and moon, to review the various approaches that have been employed in approximating the trajectories, and to select a "standard" approach that offers the greatest simplicity and convenience without undue sacrifice of realism and accuracy. In carrying out these investigations, a new method of approximation was evolved, and this method will be described and evaluated in the discussion that follows.

Development of Method

Basic Considerations

The basic problem of low-thrust transfer between satellite orbits of the earth and moon can be characterized rather aptly in terms of an analogy based on the potential well idea. The starting earth satellite orbit would be represented at a position low in the potential well of the earth. The immediate objective would be to impart energy to the vehicle as rapidly as possible (which at best would be comparatively slowly with a power-limited vehicle), until the vehicle has gained enough energy to travel across the potential ridge leading to the lunar well. Then the remaining task consists essentially of reducing energy to produce the desired descent into the potential well of the moon (low satellite orbit).

Thus the problem is primarily one of energy change, first an increase and then a decrease. If one assumes a constant (except for possible zero-thrust coasting periods) thrust magnitude, as is done in the present study, the question of how to produce the desired energy changes most efficiently reduces to one of selecting the optimum thrust direction program. Since it is known that tangential (to the trajectory) thrust maximizes the instantaneous rate of change of energy, then the constant tangential thrust program is the obvious choice† for the present application. The steering program consists simply of holding the thrust vector parallel to the velocity vector during ascent maneuvers and antiparallel during descent maneuvers.

Presented as preprint 65-87 at the AIAA 2nd Aerospace Sciences Meeting, New York, N. Y., January 25–27, 1965; revision received April 7, 1965. The author is indebted to Raymond Smith of the Marshall Space Flight Center (MSFC) Computation Laboratory for his assistance in programing and carrying out the machine computations involved in this study.

* Aerospace Engineer, Research Projects Laboratory. Member AIAA.

† Although not strictly optimum for the over-all maneuver, it is sufficiently close. For further discussion of this subject see Ref. 6 and p. 15 of Ref. 7.

Trajectory Synthesis

A typical constant tangential thrust ascending spiral is shown in Fig. 1. All but the last few turns are omitted from the figure because of their large number and very close spacing. At the end of the powered spiral, the figure shows an arbitrarily selected thrust cutoff point and also the elliptical ballistic path that the vehicle would follow after such a cutoff. It is seen that the vehicle coasts to a maximum distance (apoapsis) determined by its kinematic state at cutoff. The same figure also serves to show the general characteristics of a descending spiral and its coasting arc, if the direction of travel and sequence of events are reversed.

It is apparent that two such spirals, an ascending one about the earth and a descending one about the moon, can comprise the principal building blocks for the composite earth-moon trajectory desired. The main problem is to find a suitable method of joining them. It should be recalled in this connection that the basic reason for considering low-thrust advanced propulsion in this application is to obtain propellant economy. It therefore seems desirable to take advantage, if possible, of the previously mentioned coasting potentiality in forming the connecting trajectory segment. One possibility for doing this appears upon noticing that the angular orientation of each spiral in its plane is entirely arbitrary. It is possible, for example, in visualizing the moon in its orbit about the earth and the geocentric and selenocentric spirals superimposed about their respective centers, to have both coasting apoapsides fall on the earth-moon line. In theory, this orientation is accomplished simply by selecting the proper start-up point in the original earth satellite orbit and allowing the final cutoff point in the lunar satellite orbit to fall as required by the approach orientation chosen. Furthermore, it is possible to cause the two apsides to fall at the same point on the earth-moon line, since the apsidal distances of each vary continuously as a function of thrust duration.

Figure 2 shows a composite trajectory formed by the technique just described. Perhaps the most distinguishing feature of such a composite is the fact that the coasting arc junction falls on the earth-moon line (because of the tangential joining of *apsides*); for that reason, the general procedure will be referred to hereafter as "collinear matching." The joining of apsides is seen to be a feature in common with the familiar Hohmann-type transfers. Some similarity can also be noted in the low-thrust interplanetary trajectories of Fox,[8] which also are synthesized by comparing the osculating orbits associated with powered phases initiated at the two terminals. Fox's approximation involved only a single conic segment (with nonapsidal extremities), however, since only the sun's field was involved.

To summarize the basic scheme depicted in Fig. 2, the simulated flight begins with the start-up of the low-thrust engine in the initial orbit, followed by an extended propulsion period during which the vehicle spirals outward to the cutoff point C. It then coasts to the apsis A. Up to this point, the vehicle is attracted only by the earth. At A the vehicle passes through the "gravity field partition" and thereafter is influenced only by the moon. It coasts along the selenocentric ellipse to the start-up point S, after which it is under reverse tangential thrust until circularity at the desired altitude above the moon is reached. In relation to a real transfer trajectory, the principal assumption here is that the composite coasting arc C-S is sufficiently similar (actually, having similar terminal states) to a corresponding true coasting arc in the physical earth-moon system.

Velocity Compatibility and Matching Modes

In the scheme just described, however, there is one requirement that has not yet been considered. It is that, in addition to the requirement for coincidence of the two apsides, the vehicle velocities at those points must be compatible. This situation is not likely to occur for a random pair of cotangential coasting ellipses, but recalling the line of reasoning followed earlier in regard to the apsidal distances, it can be inferred that each pair of ellipses is but one member of a continuous family of such pairs. Again, the thrust durations determine the apsidal distances and, in turn, the particular pair of ellipses generated. The crucial test is in determining whether one of these pairs exhibits the velocity compatibility required.

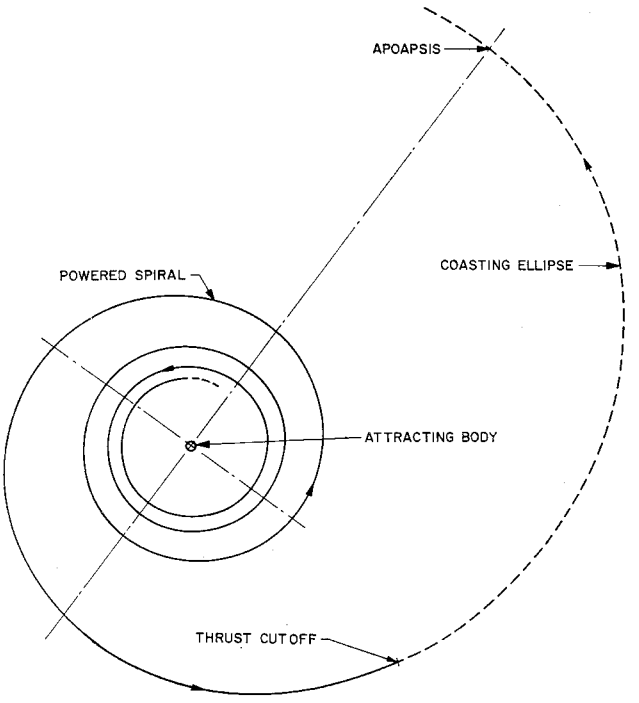

Fig. 1 Typical low-thrust ascent spiral with thrust cutoff and coast.

In order to explore the apsidal matching possibilities systematically, it is desirable to use a more general approach than the somewhat intuitive one previously followed. The general objective is to isolate pairs (one geocentric and one selenocentric) of coasting ellipses which have compatible

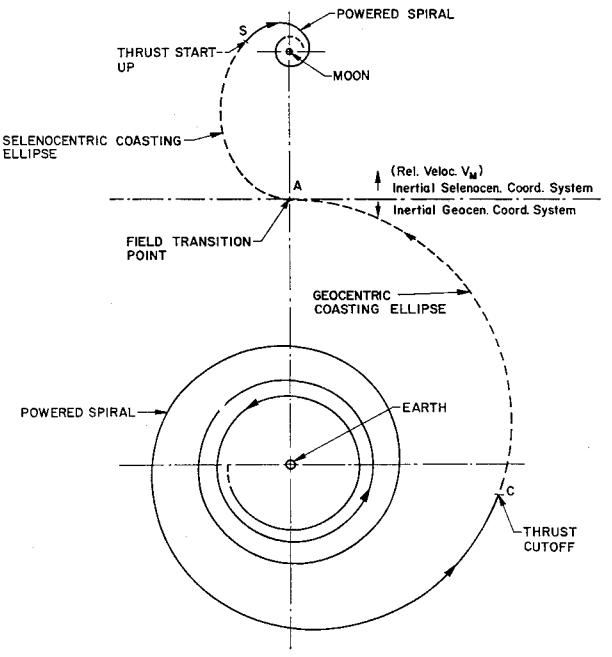

Fig. 2 Typical composite trajectory (cislunar match).

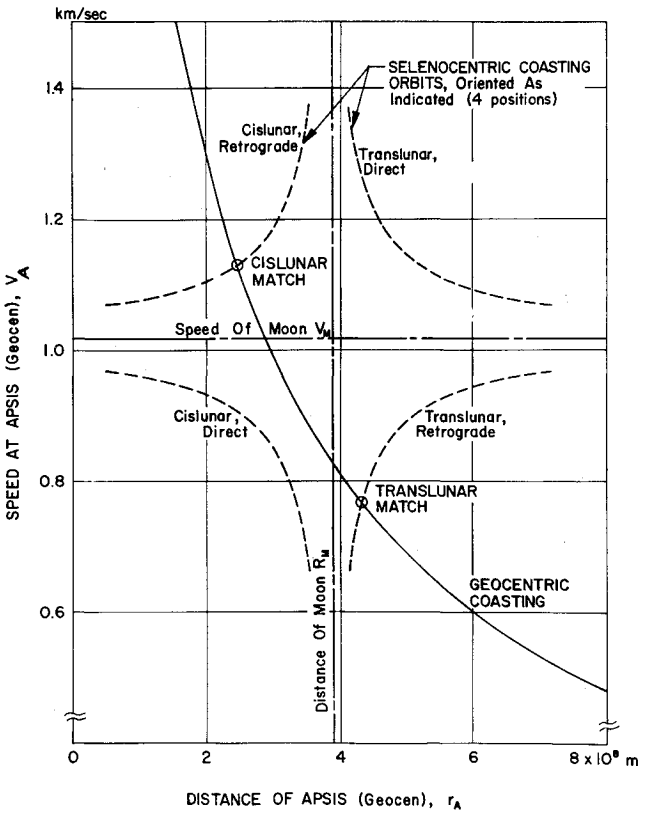

Fig. 3 Compatibility of collinear apoapsides.

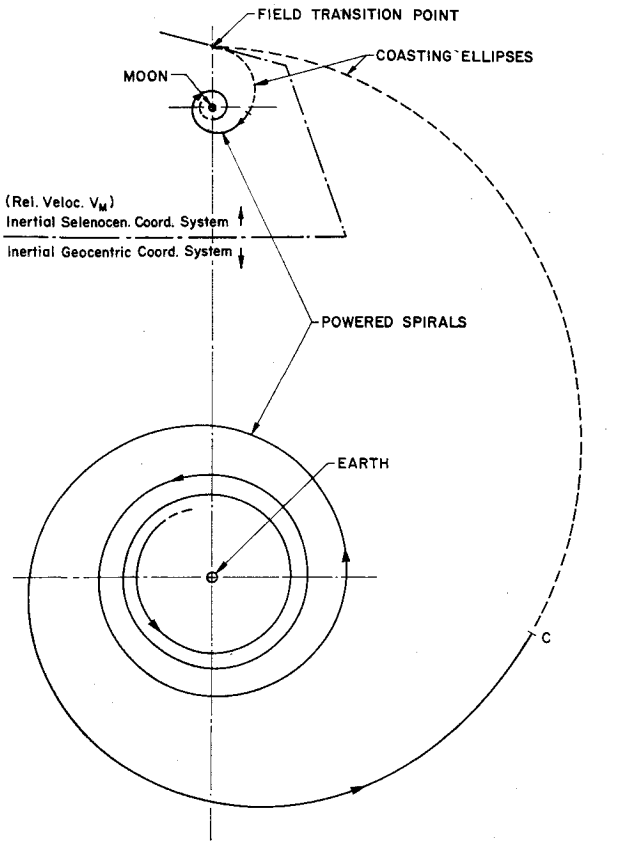

Fig. 4 Typical composite trajectory (translunar matching mode).

kinematic states (position and velocity) at their apoapsides. The word "compatible" has been used in this connection rather than "same" because in practice, the geocentric and selenocentric trajectory segments will be generated separately in inertial coordinate systems. For the matching comparison, the selenocentric apsidal states will then be transformed to the geocentric coordinate system by adding the actual relative motion of the moon. In considering this transformation, it becomes apparent that there is more than one mode to be explored. In addition to the arrangement shown in Fig. 2, in which the common apsis falls between the earth and moon, it may be possible to find suitable common apsides beyond the moon. Furthermore, although a clockwise (retrograde, assuming viewing from the north) selenocentric trajectory is shown in Fig. 2, a counterclockwise trajectory would be equally admissible.‡ Thus four possible modes exist, corresponding to the different combinations of cislunar and translunar matching locations with the direct and retrograde lunar trajectories.

Probably the most convenient and straightforward method of investigating these matching possibilities is one using a graphical procedure. Under the restrictions stated or implied so far, only two scalar variables actually remain to be compared. These are radial distance (r_A) and speed (v_A) at the coincident apsides. The other variables are accounted for as follows: 1) a planar geometry is assumed, 2) the angular position of the apsides is fixed by confining it to the earth-moon line, and 3) the direction of velocity at an apsis is by definition perpendicular to the radius vector, and consequently in this case perpendicular to the earth-moon line. Thus for the required comparisons, it is necessary only to plot v_A vs r_A for the geocentric and selenocentric coasting ellipses on the same pair of axes, as is done in Fig. 3. The solid curve traces the changing properties of the geocentric coasting ellipses as the thrust duration of the parent spiral is increased. The four dotted curves are based on a similar history generated from a selenocentric spiral. The selenocentric curve assumes four different orientations corresponding to the four matching modes described earlier. In practice, the process of transforming the selenocentric apsis data to the geocentric coordinate system involves only adding or subtracting the earth-moon distance (R_M) and the orbital speed of the moon (V_M), which accounts for the symmetry of the four dotted curves in Fig. 3 about the R_M and V_M lines.

The most significant features of Fig. 3 are the two intersections (shown encircled). These indicate that two compatible pairs of coasting ellipses actually occur, one between the earth and moon and one beyond the moon. Both are associated with retrograde selenocentric spirals. A composite trajectory based on the translunar intersection is illustrated in Fig. 4; the cislunar mode was shown previously in Fig. 2. The direct lunar spirals do not produce intersections and must be ruled out. Based on the intersections of the retrograde ellipses, however, the workability of the collinear matching method is now assured, subject only to the usual questions as to the degree of approximation to real trajectories in physical earth-moon space.

The discussion so far has assumed the earth-to-moon direction of travel in several places where it was convenient to use a specific direction for illustration. It should be emphasized, however, that the basic scheme is reversible, and it therefore applies equally well to earthbound and round trip trajectories also. In general configuration, corresponding moonbound and earthbound trajectories would appear mutually symmetrical about the earth-moon line (the earthbound versions of Figs. 2 and 4 formed as mirror images of those figures).

‡ This statement bears on a subject outside the scope of the present study, namely, the high-thrust shuttle operation between the lunar surface and the lunar satellite orbit. This shuttle operation will be a necessary part of an over-all logistic scheme based on low-thrust vehicles, and it will be constrained to use as a terminal the same lunar satellite orbit as the low-thrust vehicle. Because of the low rotational rate of the moon, however, the lunar azimuth along which take-off and landing occur is considered unimportant, and the direction of motion in the lunar satellite orbit is therefore unrestricted.

Numerical Application and Results

In order to carry out a numerical test and evaluation of the collinear matching method, a number of calculations were performed for selected specific cases. Essentially, these calculations consist of a series of high-speed computer runs combined with various manual operations for matching the machine runs and evaluating the results. The computer calculations are concerned primarily with the numerical integration of the powered spirals, using equations of motion expressed as follows:

$$\ddot{r} - r\dot{\theta}^2 = -K/r^2 + f\dot{r}/[\dot{r}^2 + (r\dot{\theta})^2]^{1/2} \quad (1)$$

$$r\ddot{\theta} + 2\dot{r}\dot{\theta} = f\,r\dot{\theta}/[\dot{r}^2 + (r\dot{\theta})^2]^{1/2} \quad (2)$$

where

$$f = F/m = c/[(c/f_0) \pm t] \quad (3)$$

Equations (1) and (2) are simply the standard equations of motion in polar coordinates of a body under the influence of a Newtonian gravitational field and a constant tangential thrust (the final term in each equation). The normal form of Eq. (3) carries the minus sign, which causes the thrust acceleration to increase with time as expected for a vehicle under constant thrust but decreasing in mass. The alternate plus sign shown is used in integrating the descending trajectories, which are generated most conveniently by "backward" integration.[8, 9] This technique allows the integration to begin at the known final state (circular orbit§) and proceed in the reverse (ascending) direction. When the vehicle motion is later interpreted as having occurred in the opposite direction, the thrust acceleration increases with time in the correct manner.

The families of coasting arcs are calculated and displayed conveniently along with the powered trajectory data output, because each such arc describes the path that the vehicle would follow if the thrust were terminated at that instant. It is the Keplerian orbit that corresponds to the state of the vehicle at the given instant, sometimes called the "osculating" or "instantaneous" orbit. In the present application, the desired properties of these orbits are r_A, v_A, and T_{RC}, which can be calculated using the following relations:

$$r_A = p/(1 - \epsilon) \quad (4)$$

$$v_A = [h(1 - \epsilon)]/p \quad (5)$$

$$T_{RC} = (\pi - M)/n \quad (6)$$

The intermediate quantities in the foregoing equations are obtained from the integrated values of the state variables via the standard equations for Keplerian motion (conic relationships, Kepler's equation, etc.).

Before specific cases can be investigated, it is necessary to make quantitative assumptions regarding the propulsion system. The earlier choice of constant tangential thrust actually left open two performance parameters that influence the trajectories. These are thrust acceleration and specific impulse. It is evident from Eqs. (1) and (2) that the thrust acceleration f is the primary quantity from the standpoint of flight mechanics. Specific impulse (or equivalently, exhaust speed c) enters the equations only through its influence on f; in effect, the value of c determines how rapidly f rises from its initial value f_0. In the presentation of results to follow, therefore, the various quantities of interest will be displayed as functions of thrust acceleration. More specifically, the average value of thrust acceleration ($\langle f \rangle$, defined as $\Delta v/t$) will be used as the argument, since it is representative of the range of the variable f over a given trajectory.

A very useful analytical approach to the numerical work is to evaluate cases in which f is held constant. Although the constant thrust constraint applied earlier makes this case a theoretical limit only ($c \to \infty$), the technique eliminates one parameter from the analysis (specific impulse), and the resulting performance provides a useful guide in analyzing the results of practical cases.¶

Velocity Increments

Assuming that the prime application of the present study is in estimating propulsion requirements, the most important results are presented in Fig. 5. This figure displays velocity increments derived from the trajectory calculations as a function of the argument chosen above ($\langle f \rangle$). Velocity increment ($\Delta v = \int f\,dt$) is chosen to represent propulsion requirement because it is easily calculated and it defines the propellant expenditure (for a given c) associated with a constant thrust trajectory. The curves in Fig. 5 show a small difference in Δv for the two matching modes, and they show the expected fall off of required Δv as the acceleration level increases.

The results for the limiting constant-acceleration case, which was discussed in the previous section, are shown by the two solid curves. The "real" data, for finite values of specific impulse, appear in similar patterns below and above the solid curves, with the direction of the offset determined by the direction of travel (moonbound and earthbound,

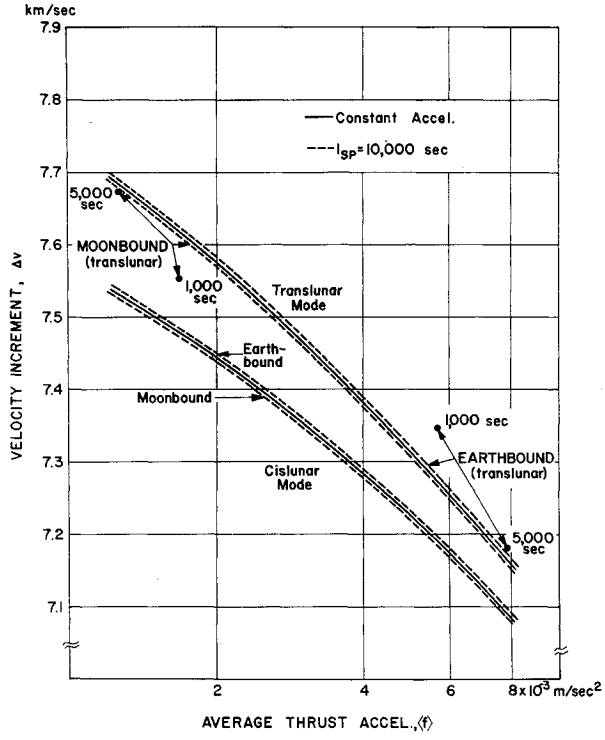

Fig. 5 Velocity increment variations (one-way).

§ Terminal orbit altitudes of 500 km at the earth and 100 km at the moon are used throughout the present numerical studies. The respective gravitational parameters assumed are 3.986×10^{14} and 4.890×10^{12} m³/sec². A circular lunar orbit of 3.844×10^8 m radius is assumed.

¶ The constant-acceleration case is also easier to handle numerically, because identical acceleration values are used in initiating the two computer runs to be matched for a given composite. In the finite-c case, however, it is necessary to estimate and allow for acceleration changes along the two powered spirals, so that the acceleration values at the two extremities of the coasting arcs will correspond. Such estimates can be made using escape time requirements [based on approximations such as Eq. (28) in Ref. 7] as rough guides in estimating propulsion durations, or, more conveniently, using specific information reported herein (Figs. 5 and 9).

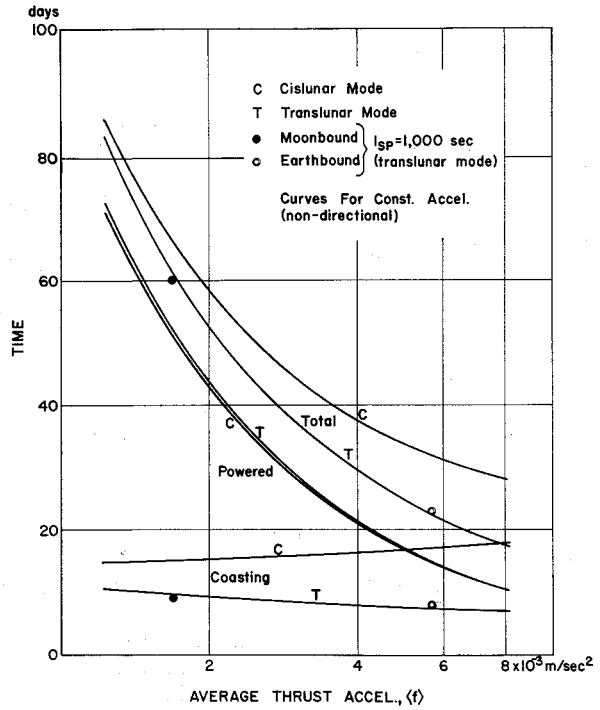

Fig. 6 Flight times (one-way) vs acceleration.

respectively) of the vehicle. This characteristic of the data is a result of the asymmetry, produced by acceleration variations, between the moonbound and earthbound trajectories at finite values of specific impulse. Only under constant acceleration are the moonbound and earthbound trajectories symmetrical, as indicated by the single, nondirectional curves representing those cases.

It is also noteworthy in Fig. 5 that the quite substantial change from 10,000 to 5000 sec specific impulse produces an almost insignificant change in velocity increment, and even a change to 1000 sec does not produce an effect comparable to the variations associated with average acceleration.

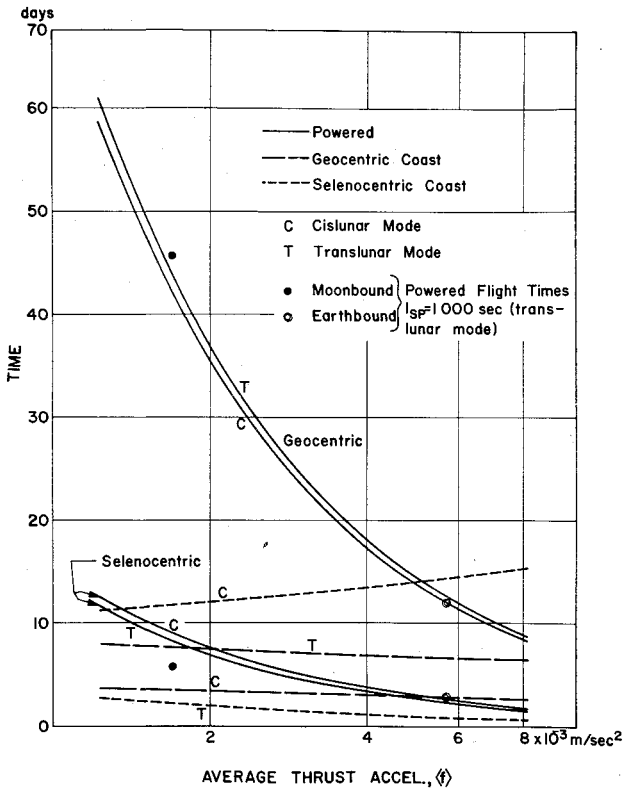

Fig. 7 Flight times for individual trajectory segments.

Flight Times

The second most important quantity in the over-all results is considered to be flight time. This assessment, assigning a secondary importance to the time factor, is based on the assumption that low-thrust flights to the moon will be made primarily to transport heavy cargo, for which the transfer time will not be critical. The desired cargo flow rates would be obtained simply by having enough vehicles in operation at the same time. Under these assumptions, the main influence of flight time would be in determining the number of trips possible within the operating lifetime of a particular vehicle.

The over-all flight-time data derived from the numerical studies are summarized in Fig. 6. The figure shows that the powered flight times do not vary appreciably with the choice of matching mode, as would be expected from the closeness of the corresponding Δv curves in Fig. 5. The coasting times, however, show substantial differences, particularly at the higher accelerations, and these differences are of course reflected as a sizeable divergence between the total transfer time curves. All of the curves shown in Fig. 6 and subsequent figures are based on constant-acceleration results; a few finite-I_{sp} points are indicated for comparative purposes.

The basic data of Fig. 6 are re-presented in greater detail in Fig. 7. In this figure, the flight times associated with each segment of the composite trajectory are shown individually. Again, the powered flight-time patterns are not surprising. Perhaps the most noticeable aspect of the figure is the relatively long durations shown for the selenocentric coasting phase in the cislunar mode. These times rise to about 15 days, compared to less than 3 days for the translunar mode.

Comparisons to Other Methods and Results

Approximation Problem

As with all methods of approximation, some means must be found for estimating the errors involved, and the lack of optimum thrust programs and trajectories for use as standards for comparison was noted previously. So far as the powered trajectory phases are concerned, however, the use of tangential thrust for escape and capture-type maneuvers is well established, and the powered spirals do not extend into the regions of strong third-body effects. The coasting arcs require further consideration, however. Although their exact properties probably do not affect propulsion requirements greatly, they are substantially involved in determining the over-all flight times. For that reason, an independent "standard" for comparison was sought for the coast approximations. The choice of an alternate scheme was limited, by practical considerations, to those that involve only two-body methods.

There are several approaches to the general question of how to effect the transitions between the various two-body phases in approximations to multibody problems. This subject seems rather poorly defined, which would be expected to some extent because of the varying criteria by which such approximations are to be judged. In one case the criterion might be geometric similarity to the real trajectory (a feature which itself needs further definition), whereas, in other cases, velocity, energy, angular momentum, or flight time may be of the most direct interest. Hence the proper choice of transition method may vary among particular applications.

The classical transition scheme is based on the "activity sphere" or "sphere of influence" concept, which apparently dates back at least to Laplace (1736–1827).[10] This spherical

or nearly spherical surface defines a geometric boundary between the two-body phases, and the resulting method of approximation is still used very extensively. Certain other methods have been employed recently, including attractive ones reported by Lagerstrom and Kevorkian[11] and by Martikan et al.[12] The latter reference defines a new region, called the "volume of influence," which was determined empirically to yield good approximations to the ballistic lunar trajectories described in the reference.

Comparison to Activity Sphere Matching Method

In view of the time-tested reliability and standard usage of the activity sphere matching method, the existing instances of its successful application in earth-moon space,[13,14] and its use by London[1] for low-thrust lunar trajectories, this method was adopted as the alternate procedure to be used for the desired comparisons. The detailed procedures employed are believed to be similar to those used by London, and the results obtained correspond closely.

Velocity increment values determined using the activity sphere matching method with constant thrust acceleration are shown in Fig. 8. As with collinear matching, two possible modes are evident, but the distinction in this case is in the selenocentric direction of motion (which is retrograde for both modes in collinear matching). Although the two activity sphere modes appear to be equally admissible in principle, the direct mode is chosen for the comparisons herein because of its more favorable Δv requirement (the coasting times do not differ greatly, as will be shown).

For comparative purposes, the constant acceleration curves of Fig. 5 (collinear matching) are reproduced in Fig. 8. Good correlation (within 1% over most of the $\langle f \rangle$ range) is evident between the collinear translunar mode and the activity sphere method (direct mode).** This comparison is especially interesting in view of the sizeable distances between the activity sphere location and the transition points in collinear matching. For the acceleration range considered, the collinear transition locations are situated earthward from the activity sphere intercepts†† on the earth-moon line by about 71 to 116 Mm for the cislunar mode and 17 to 46 Mm for the translunar mode (the displacements increase with acceleration level). The comparisons suggest that considerable latitude is available in the choice of transition regions in such approximations.

Figure 9, which is self-explanatory, provides further details concerning relative propulsion times associated with the two methods of approximation.

Comparisons to Published Results

Figure 8 also shows two data points derived by applying standard rocket relationships to the data given in Table I of Ref. 1. These points, as expected, fall close‡‡ to the curve for the new activity sphere data. Also indicated in Fig. 8 is the single Δv value adopted for performance studies in

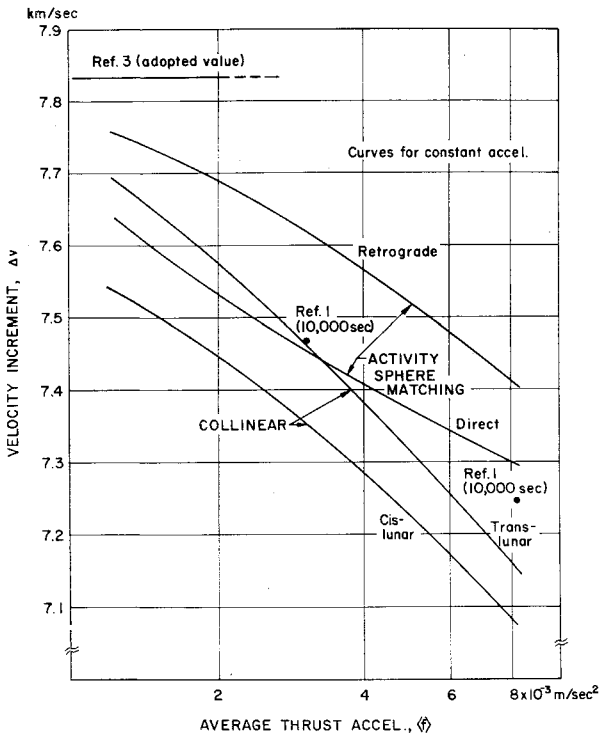

Fig. 8 Velocity increment comparisons.

Ref. 3. This value is also quite compatible with the present results if it is interpreted as a probable maximum for the thrust acceleration ranges of practical interest. As to methods, Ref. 3 indicates the use of transverse (circumferential) thrust for earth escape, and several different steering programs, applied in sequence to modify specific trajectory properties, for the lunar approach and descent maneuvers. Reference 3 defines two spatial boundaries, based on force comparisons, in connection with the field transition require-

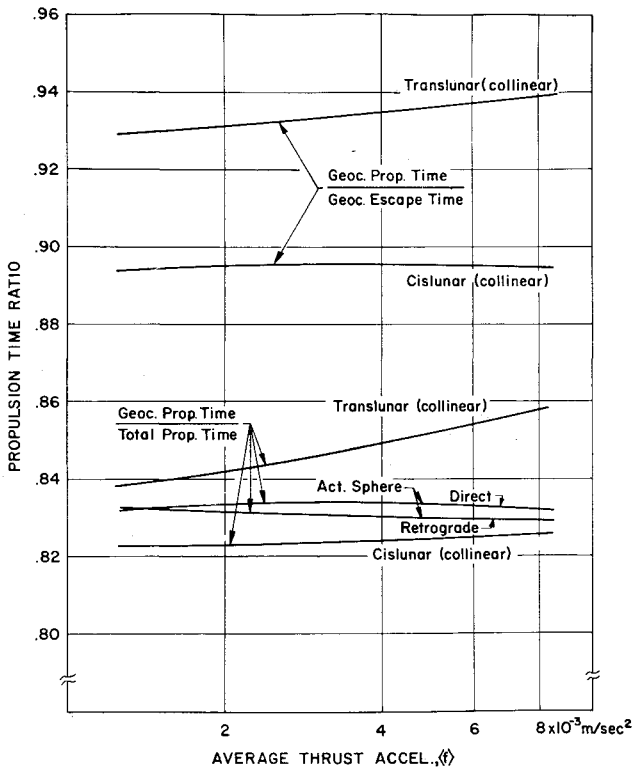

Fig. 9 Propulsion time ratios in collinear and activity sphere matching.

** The following example illustrates the detailed relationship between the two methods. For a constant thrust acceleration of 1.372×10^{-3} m/sec², the collinear method (translunar mode) involves geocentric and selenocentric propulsion times of 54.3 and 10.4 days, respectively. The corresponding trajectory with activity sphere matching embodies the same pair of powered spirals, but the geocentric one is shortened by 0.80 days, and the selenocentric one is extended 0.34 days (and rotated). These differences yield a net propulsion time decrease of 0.7%.

†† The activity sphere applied herein is a true selenocentric sphere of 66,133 km radius.

‡‡ Compensating for the higher terminal orbit altitudes (10% of the respective surface radii) used by London moves the two points upward about 0.1 km/sec from the positions shown. No other altitude differences were detected; which affect the literature comparisons significantly.

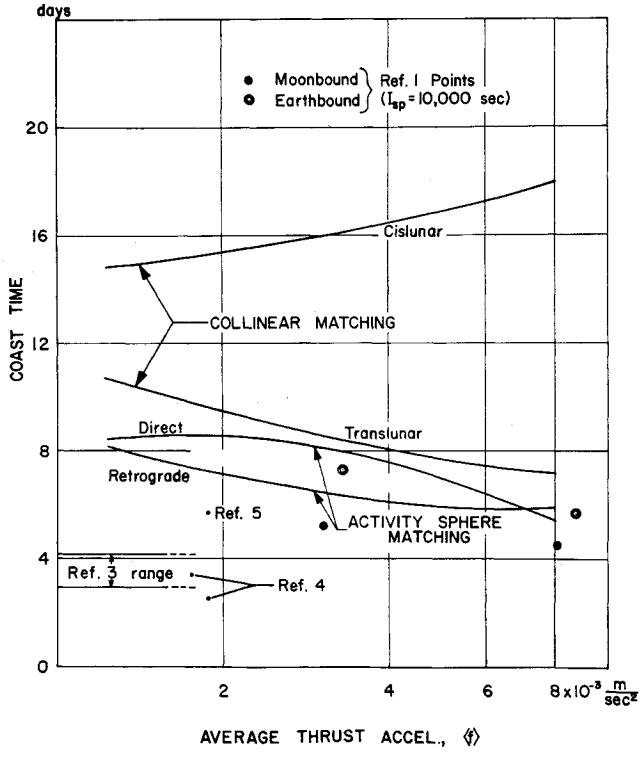

Fig. 10 Coasting time comparisons.

ment and confines the transition point to the finite zone between the boundaries.

No further meaningful comparisons of propulsion requirements were obtained from the literature. The flight profile assumed by Stuhlinger[2] was of the lunar flyby (rather than orbiter) type, so that no direct comparisons were possible. The results reported by Battin and Miller[4] are not considered strictly comparable to the present ones because of basic differences of approach. As stated in the reference, the authors considered the guidance and control aspects of the lunar flight problem, in contrast to the ideal or "reference" trajectory determination problem usually treated. Accordingly, they formulated several guidance policies to be followed during different phases of the flight and applied these in machine-simulated flights. This approach, as might be expected, yielded propulsion requirements moderately greater than the present methods, by about 8% according to rough calculations based on the data reported.

The lunar flight analyses of Ref. 5 appear to employ methods comparable to the present ones, including constant tangential thrust for escape maneuvers (but modified for powered descents) and an activity sphere approach to the transition point selection. Efforts by the present author to reconcile the propulsion data reported were not successful, however, in that the velocity increments derived appeared unrealistically high.

As suggested earlier, the largest differences in results between the various trajectory approximation methods occur in the coasting times. This situation is illustrated by Fig. 10, which reproduces the coasting time curves of Fig. 6 on a larger scale. Also shown in Fig. 10 are curves for the coast periods associated with the two modes of activity sphere matching, along with various values taken or derived from Refs. 1 and 3–5. In view of the general dispersion of these values, only the cislunar mode (collinear) results appear prominently displaced from the over-all pattern. Values for the translunar mode are reasonably compatible with those obtained by activity sphere matching (direct mode). The values from the literature are generally somewhat lower. The longest coasting time found in the references was 8 days (Ref. 1, at $f_0 = 2.94 \times 10^{-4}$ m/sec^2 and $I_{sp} = 2000$ sec). In the over-all consideration of the coast phases, however, it should be remembered that these ballistic arcs are rather sensitive to small changes in injection conditions (low-thrust cutoff). In general, the coasting phase can be eliminated entirely with moderate increases in propulsion time.

Evaluation and Summary

As a practical means of estimating the characteristics of low-thrust lunar flights, the translunar mode of collinear matching appears generally preferable to the cislunar mode. It provides slightly more conservative estimates of propulsion requirements, it yields shorter flight times (because of shorter coasts), and it avoids the larger transition point excursions previously noted in "Comparison to Activity Sphere Matching." The eventual use of lower acceleration ranges than those considered here, as some observers of advanced propulsion developments might now predict, would tend to reduce the transition point excursions in both modes.

The velocity increments (and powered flight times) defined by the translunar mode are expected to be near the minimum values obtainable. This opinion is based on confidence in the approaches applied in developing the approximation method, and on the fact that the numerical values obtained are generally comparable to or lower than those available from other sources. The coasting times indicated may be a few days longer than would be used in actual missions, but such differences are not considered very significant. Experience would indicate that coast time reductions, if desired, could be obtained rather inexpensively, perhaps by suitable propulsion programs inserted near the extremities of the coasting arcs.

In the area of general observations, it should be noted that many of the methods applied herein are not constrained to uses associated with low-thrust trajectories. The simplicity and convenience of the collinear matching method could prove helpful in other applications, including those involving high-thrust vehicles. This possibility might bear further investigation, and some general and definitive work on the design of two-body approximations is certainly in order. It is also clear that the optimality of low-thrust trajectories in earth-moon space needs to be investigated systematically.

References

[1] London, H. S., "A study of earth-satellite to moon-satellite transfer using non-chemical propulsion systems," United Aircraft Corp. Rept. R-1383-1 (May 21, 1959).

[2] Stuhlinger, E., "Lunar ferry with electric propulsion system," Proceedings of First Symposium (International) on Rockets and Astronautics, Tokyo (1959).

[3] Brown, H. and Nicoll, H. E., Jr., "Electrical propulsion capabilities for lunar exploration," AIAA J. **1**, 314–319 (1963).

[4] Battin, R. H. and Miller, J. S., "Trajectories and guidance theory for a continuous low-thrust lunar reconnaissance vehicle," *Proceedings of the Sixth Symposium on Ballistic Missile and Aerospace Technology* (Academic Press, Inc., New York, 1961).

[5] Donham, J. J. and Golden, C. J., "Mission analysis for space vehicles powered by low acceleration, power-limited propulsion devices," Lockheed Missiles and Space Co., Aeronautical Systems Div. Rept. ASD-TDR-62-1060 (January 1963).

[6] Irving, J. H., "Low-thrust flight: Variable exhaust velocity in gravitational fields," *Space Technology*, edited by H. Seifert (John Wiley and Sons, Inc., New York, 1959), pp. 10–21.

[7] Melbourne, W. G., "Interplanetary trajectories and payload capabilities of advanced propulsion vehicles," Jet Propulsion Lab. TR 32-68 (March 31, 1961).

[8] Fox, R. H., "Powered trajectory studies for low-thrust space vehicles," ARS Preprint 879–59 (June 1959).

[9] Moeckel, W. E., "Trajectories with constant tangential thrust in central gravitational fields," NASA TR R-53 (1960).

[10] Tisserand, F., *Traité de Méchanique Céleste, Tome IV* (Gauthier-Villars, Paris, 1896), Chap. XII.

[11] Lagerstrom, P. A. and Kevorkian, J., "Numerical aspects of uniformly valid asymptotic approximations for a class of trajectories in the restricted three-body problem," *AIAA Progress in Astronautics and Aeronautics: Celestial Mechanics and Astrodynamics*, edited by V. G. Szebehely (Academic Press, New York, 1964), Vol. 14, pp. 3–34.

[12] Martikan, F., Emery, L., Santora, F., Garceau, T., and Jazwinski, A., "Trajectories in the earth-moon system," *Lunar Flight Handbook* (Martin Co., Baltimore, Md., 1963), Chap. IV.

[13] Egorov, V. A., "Certain problems on moon flight dynamics," *The Russian Literature of Satellites, Part I* (International Physical Index, Inc., New York, 1958), pp. 115–174.

[14] Dallas, S. S., "Moon-to-earth trajectories," Jet Propulsion Lab. TR 32-412 (June 1, 1963).

AUGUST 1965 AIAA JOURNAL VOL. 3, NO. 8

Necessary Conditions for Singular Extremals

RICHARD E. KOPP* AND H. GARDNER MOYER†
Grumman Aircraft Engineering Corporation, Bethpage, N. Y.

The purpose of this paper is to derive a set of necessary conditions for singular arcs. In this case, the classical Weierstrass and Legendre tests as well as the maximum principle fail to determine the nature of the extremal path. In the present analysis the second variation of the function to be minimized is evaluated for explicitly defined control variations. The dominant term of a power series in τ, a parameter of the control variation which is allowed to approach zero in the limit, is calculated and examined for semidefiniteness. Should this term be zero for a particular problem, a new control variation is chosen and the procedure repeated. These control variations all belong to a special class of functions that were constructed with the satisfaction of terminal boundary conditions in mind. These boundary conditions are satisfied by applying secondary control variations that contribute terms to the second variation that are at least one degree higher in τ. The results of the analysis are applied to the specific problem of rocket flight in an inverse square law field. It is shown that, for the time open case, the singular arc (Lawden's spiral) is nonoptimal.

Introduction

SINGULAR extremals are usually associated with variational problems in which the control variables appear linearly in the system differential equations. A singular arc or subarc occurs when the pseudo-Hamiltonian function H is not explicitly a function of the control variable over a nonzero interval of an extremal arc. When such a situation exists, neither the maximum principle nor the classical variational theory provides necessary conditions for the arc to be minimizing.

Several papers have discussed specific examples that exhibit singular arcs and methods of analysis.[1–5] The approach taken here is a rather general one that could be considered as an extension of Kelley's work.[3] The positive semidefiniteness of the second variation of the payoff function is examined for a special class of explicitly defined control variations. When the first member of this class is used as a control variation the results are identical with that presented in Ref. 3. However, if the inequality of the test is met marginally (equality), in which case the test is inconclusive on the nature of the extremal arc, the second special control variation in the class is used and again the positive semidefiniteness of the second variation examined. If this test should also be satisfied marginally, the third control variation may be used and so on.

In the final analysis the second variation of the payoff function is evaluated as a power series in τ for a control variation that is a general member of the class of special control variations.‡ The variable τ is a parameter of the control variation which is allowed to approach zero in the limit. Each successive term in the power series provides a sequence of necessary conditions, each successively being applicable when the former is identically equal to zero. The general term of the series is expressed recursively as a function of the previous term. The special class of control variations has been constructed so that terminal conditions can be satisfied by an additional control variation that contributes terms to the second variation which are at least one degree higher in τ.

Although not apparent, it is shown in the appendix that the sequence of necessary conditions can be restated concisely as $(-1)^k(\partial/\partial u)(d^{2k}/dt^{2k})H_u \geq 0$. This expression is a generalization of the Legendre condition for nonsingular extremals and was first obtained independently in this form by Robbins. Although the expression given in the foregoing is a more concise statement of the sequence of necessary conditions derived in this paper, its derivation lacks some of the motivation of the former development and is thus delegated to the appendix. The actual application of the equivalent tests involves about the same amount of computation.

Problem Formulation

The problem is formulated as a Mayer problem; that is, given a system of differential equations and specified boundary conditions

$$\begin{aligned} \dot{x}_i &= f_i(x_1, \ldots, x_n, u_1, \ldots, u_r, t) \qquad i = 1, \ldots, n \\ x_i(0) &= x_{i0} \qquad i = 1, \ldots, n \\ x_i(t_f) &= x_{if} \qquad i = 1, \ldots, m \qquad m \leq n \end{aligned} \tag{1}$$

Presented as Preprint 65-63 at the AIAA 2nd Aerospace Sciences Meeting, New York, N. Y., January 25–27, 1965; revision rereceived April 29, 1965. This work was partially supported by the Air Force Office of Scientific Research of the Office of Aerospace Research, under Contract No. AF49(638)-1207.

* Section Head, Systems Research. Member AIAA

† Research Mathematician. Member AIAA

‡ It has been tacitly assumed in the analysis to follow that the power series in τ for the second variation of the payoff functional has a nonzero interval of convergence.